Journal of Information Systems Engineering and Management
2025, 10 (29s)
e-ISSN: 2468-4376
https://jisem-journal.com/

Research Article

Implementation of ANFIS-Based PID Controller in a Three-Phase Solar PV-Integrated UPQC for Power Quality Improvement

Kumar Saliganti[1*], Papana Venkata Prasad[2], Erukula Vidyasagar[3]
[1,3]*Department of Electrical Engineering, University College of Engineering, Osmania University, Hyderabad, Telangana, India*
[2] *Department of Electrical and Electronics Engineering, Chaithanya Bharathi Institute of Technology, Hyderabad, Telangana, India*
Email: [1] skjntum@gmail.com, [2] pvprasad_eee@cbit.ac.in, [3] vidyasagar.e@uceou.edu

ARTICLE INFO

Received: 22 Dec 2024

Revised: 22 Feb 2025

Accepted: 28 Feb 2025

ABSTRACT

The incorporation of renewable energy sources into the grid presents challenges like reactive power compensation, harmonics, voltage sags, and swells, which impact power quality. This paper proposes a single-stage PV-linked Unified Power Quality Conditioner (PV-UPQC) for a three-phase grid-connected system to address these issues while optimizing PV energy utilization. The system employs Perturb and Observe (P&O) MPPT for maximum power extraction and an Adaptive Neuro-Fuzzy Inference System (ANFIS)-based PID controller for dynamic inverter switching, ensuring precise tuning and adaptability. Simulation analyses under various load scenarios and grid disturbances demonstrate the system's capability to enhance power quality. The ANFIS-PID controller achieves superior performance with balanced gain values (K_p = 1, K_i = 1, K_d = 0.01), reducing steady-state error and improving response time. It maintains a refined DC link voltage range of 660–700 V, outperforming other methods. The outcomes verify that the proposed PV-UPQC system effectively integrates renewable energy, stabilizes voltage, and mitigates power quality issues, making it an ideal solution for modern grid-connected applications.

Keywords: Solar PV-UPQC, ANFIS-PID Controller, Voltage Regulation, Harmonic Mitigation, Renewable Energy Integration, Grid Disturbances

INTRODUCTION

In the context of increasing non-conventional resources addition, maintaining power quality and stability in power systems has become essential. PV systems, while beneficial for reducing dependency on non-renewable sources, present unique challenges due to their intermittent nature, impacting grid stability and quality. To address these challenges, UPQC are widely used in power systems for mitigating problems like sags, swells, harmonics, and reactive power imbalances. Integrating UPQC with solar PV systems provides a dual advantage by enhancing power quality while promoting green energy usage.

1.1. Background & Motivation

Power quality (PQ) issues such as harmonics, voltage sags, swells, and reactive power imbalance have become significant challenges in modern power systems, especially with the increasing integration of renewable energy sources (RES) like solar photovoltaic (PV) systems. Traditional compensators often struggle to adapt to the dynamic and nonlinear nature of grid-connected systems, leading to inefficiencies in addressing PQ problems. Unified Power Quality Conditioner (UPQC) systems have emerged as a promising solution for enhancing PQ by integrating series and shunt compensators. integration into the grid.

However, the performance of these systems largely depends on the control strategies employed, which must be robust, adaptive, and capable of handling diverse grid conditions. This research is motivated by the need to develop advanced UPQC configurations leveraging PV systems and intelligent controllers like Adaptive Neuro-Fuzzy Inference System (ANFIS) to optimize performance, ensure reliable operation under varying environmental and load conditions, and support seamless renewable energy.

1.2. Literature Review

In [1], an PV-UPQC scheme is presented to increase the PQ of the 3-phase system. The PCC voltage is infused into the series VSC to reduce the PQ problems. The harmonics at load current are corrected using shunt compensator. Limitations of this study include its dependency on a single control strategy, which may limit adaptability to other disturbances or environmental fluctuations. [2] presented a PV-UPQC linked in parallel in transmission line. The paper introduced a shunt compensator that replaces the conventional MPPT requirement, adding flexibility in reactive power and harmonic compensation. The paper did not explain the control adaptability in different environmental or grid conditions.

In [3], an ANN-based controller with Soccer League Algorithm is used in PV integrated system. The controller uses a filter for phase synchronization, removing the need for additional filters or PLL. The study presented that S-ANNC is effective under various load and supply voltage conditions, outperforming GA, PSO, and GWO training methods A PV, Battery combined UPQC structure is presented in [4].

An ANN control is used to solve the PQ issues. Harmony search & Firefly algorithms are used to tune the controller parameters. The presented method reduces the THD & improves the power factor. It did not explore the reconfiguration necessity when integrating additional renewable sources or dealing with diverse grid conditions. In [5], an FOPID controller which is optimized by Amplified Slime Mould-Wildebeest Herd Optimization is used in the three-phase UPQC system. It optimized DC link voltage, gain values & PQ issues. The presented method is compared with PI and FOPID-PI controllers.

In [6], A UPQC & DVR is used in the grid linked PV, Wind system. A PI controller optimized using Sparrow Search technique is used to control the switches of the compensators, The presented algorithm has limited exploration during variable environmental condition which affects the dynamic grid environment. A FOPID controller optimized for managing PQ in a hybrid RES with UPQC in presented in [7]. The controller optimizes switching pulses to respond error values in reference and load voltages. In [8], a battery-integrated RES is linked with UPQC was presented, and FOPI was optimized with Adaptive Bald Eagle Optimization Algorithm to address the PQ issues, this work demonstrated the outcomes with rise and settling times. The study did not address the additional tuning in environments with extreme voltage variations or irregular load profiles. A dual-stage PV-UPQC scheme is presented in [9], The sequence component detection and unit vector template are used to generate switching signals to the shunt VSC. The series VSC corrects grid issues and provide optimal power.

In [10], a UPQC with PV & battery is explored. The system uses a self-tuning filter linked with a unit vector generator to handle unbalanced/distorted grid conditions without requiring a phase-locked loop (PLL). Compared to conventional SRF-PLL methods, the STF-UVG approach shows enhanced stability and performance in MATLAB simulations. In [11], a PV-UPQC system is presented with ANN control. The shunt compensator manages load harmonics and extracts energy from the PV module, while the series compensator addresses grid-side issues like voltage sag and swell. A moving average filter enhances performance by isolating the load's component using a synchronous reference frame control approach. Problems in this work includes the reliance on ANN for controller performance, which might require fine-tuning in highly dynamic conditions to avoid overcompensation or lag in response. A PV-UPQC is presented in [12], A PI controller is applied to control the series & shunt compensators of the UPQC.[13] addressed PQ issues in microgrids with RES used as Distributed Generators (DGs) to reduce reliance on traditional resources were discussed. Microgrids employing RES often face harmonics and voltage sags, issues managed with a UPQC system using instantaneous reactive power (IRP) theory for efficient operation. The UPQC, supported by RES, eliminates harmonics and stabilizes microgrid voltage through active power injected via the DC-link. In [14], a PV, battery with UPQC is presented for standalone & grid linked mode. The PV-B-UPQC's series and shunt filters, linked by a common DC link, address PQ issues while supporting clean energy generation. The scheme is tested under different circumstances, including grid unavailability and solar power fluctuations, ensuring minimal disruption to loads, the problems associated with study include challenges in managing fast transition times to maintain power flow stability, especially under abrupt grid faults, which may require enhanced predictive control strategies.

A PV-UPQC for DGs and APF is presented in [15]. The shunt compensator addressed load harmonics and maximized PV power extraction, while the series VSC handles grid voltage issues by injecting out-of-phase voltage during sags and swells. In [16], An ANN-controlled PV-UPQC system is presented, The fundamental parts of PV-UPQC are the

shunt and series voltage compensators, which are combined in parallel and series with a single DC connection. Shunt compensators are designed to balance the load current harmonics and control power through photovoltaic arrays. A moving average filter (MAF) improved synchronous reference frame management and system performance. The series voltage compensator is designed to make up for grid-side power quality issues including surges and voltage drops. At the grid, the voltage is correctly injected both in-phase and out-of-phase. In [17], a PV Integrated UPQC system for enhanced efficiency, harmonic reduction was presented. Simulations demonstrated the effectiveness of series and shunt compensators, in conjunction with MPPT, improve the system's output in terms of harmonic control and reactive power handling. A PV- UPQC system using a variable leaky least mean square procedure is presented in [18]. It eliminates the need for low-pass & moving average filters. The VLLMS algorithm efficiently addresses PQ issues, like current harmonics and power factor correction, without compromising on the regulation of the DC-link potential. The problems in this study involve potential stability issues in dynamic environments, as the VLLMS algorithm's response speed might vary depending on parameter updates and operational changes. In [19], a PV-UPQC with a 3-phase four-wire NPC multilevel inverter controlled by synchronous reference frame theory was presented. The system utilized a PI controller to maintain DC capacitor voltage balance and performs well across a range of operational conditions. The challenge of maintaining stable voltage balance in dynamic environments due to the reliance on PI controllers is an issue in this study, which might require additional tuning for varied grid conditions.[20] presented an HES integrated with UPQC, incorporating RES. The (HES-UPQC) contains a series and shunt VSC connected to a common DC-link to mitigate PQ issues from non-linear loads. A second-order integrator with frequency locking via zero-crossing detection helps maintain active current balance. The system effectively manages PQ problems by inserting voltage in or out-of-phase as required.

Harmonic distortion brought on the nonlinear power electronic components in smart devices has been shown to impair system performance and efficiency in [21]. The ANFIS-based approach uses hysteresis current control to oversee PID control and provide precise gate signals for shunt active power filters (SAPF). The power factor is improved to 0.99 and harmonic distortion is significantly reduced (92.23% to 0.49%) with a transformer-less SAPF design that reduces insertion losses. This method shows that it can improve system performance while still adhering to IEEE 519 guidelines. Variations in voltage and current are introduced into distribution networks by the installation of microgrid-generating sources [22]. An ANFIS-based distributed generator control system is introduced, allowing microgrids, storage devices, and renewable energy sources to be synchronized.

In [23], A PV-integrated UPQC using a Variable Leaky Least Mean Square (VLLMS) algorithm is introduced to address harmonic distortion and power factor issues were presented. This approach eliminates the need for traditional filters by using adaptive compensating techniques for shunt and series converters. To improve power quality while lowering sensor requirements, a novel GI-BPF-FLL control algorithm is suggested for SPV-integrated UPQC systems [24]. DC offsets are removed and basic signal components are successfully extracted by the method. The SPVUPQC system adjusts for load imbalances, current harmonics, voltage sags, and swells using DSTATCOM and DVR components. The algorithm's ability to satisfy IEEE 1159 and IEEE 519 standards is confirmed by both simulation and hardware findings, highlighting how effective it is at enhancing the voltage and current quality in distribution networks.

In [25], The use of power electronics for nonlinear load control impacts power quality at the distribution level. This study integrates PV-based UPQC with DERs to enhance power exchange and reduce converter ratings. The system employs a hybrid control strategy combining Unit Vector Template and p-q theory for effective compensation of real and reactive power. An Adaptive Neuro-Fuzzy controller enhances performance during transient oscillations, addressing challenges such as dc-link sizing. Results indicate improved fault-ride-through capabilities and robust PQ performance under various load conditions. A Solar PV-based UPQC system controlled by an ANFIS model is developed to address power quality challenges, including sag, swell, and harmonics [26]. The system utilizes bidirectional converters and a dc-link for real-time power exchange, enhancing grid resilience. A fuzzy model-based controller refines reference current generation, ensuring robust PQ improvements during transient and steady-state conditions.

The effectiveness of UPQC systems heavily relies on their control strategies, which manage the dynamic and variable conditions of grid-connected PV systems. This paper proposes an ANFIS based PID control scheme for the UPQC, leveraging the adaptability of ANFIS to improve system performance under varying conditions. By integrating ANFIS-PID with the UPQC in a three-phase configuration, this study aims to demonstrate improved voltage

regulation, enhanced harmonic suppression, and efficient renewable energy utilization. Simulation results under various conditions validate the proposed approach, highlighting its potential for modernizing grid-connected PV systems and ensuring robust power quality control in renewable-integrated smart grids.

1.3. Problem statement

Increased integration of RES-like PV systems presents both opportunities and challenges for modern power grids. While PV systems reduce dependence on non-renewable energy, their inherent intermittency can impact grid stability and power quality. To mitigate these issues, UPQCs are commonly employed to address PQ problems and reactive power imbalances. However, conventional UPQC systems often rely on static control strategies that may not fully adapt to dynamic grid and environmental conditions. Several studies have proposed enhancements to PV-UPQC systems using advanced control strategies, including artificial intelligence and optimization algorithms, to improve power quality and grid reliability. Despite these advancements, limitations remain in terms of adaptability to rapidly changing conditions, computational complexity, and integration with additional renewable sources. This study seeks to address these gaps by implementing an ANFIS-PID control strategy for PV-integrated UPQCs, aiming to enhance system resilience, improve voltage regulation, and optimize power quality under various grid-connected scenarios.

1.4. Contribution of the work

The primary contribution of this work is,

- To implement a PV-integrated UPQC in a grid-linked scheme using an ANFIS-based PID control strategy, optimizing power quality and stability.
- To evaluate the effectiveness of the proposed ANFIS-PID controlled PV-UPQC in mitigating power quality issues and harmonics under diverse grid and environmental conditions.
- To compare the performance of the ANFIS-PID controlled PV-UPQC in different operating conditions & maintain proper power balance in the system.

1.5 Organization of the paper

The paper is organized in the following sections, Section 2 presents the system configuration and design of the proposed system. The control strategy of the UPQC is presented in section 3, the results & discussions of different cases with THD & comparative analysis are presented in section-4, the section 5 shows the conclusion & future scope of the proposed work.

SYSTEM CONFIGURATION & DESIGN

The block diagram represented in Fig.1 shows a UPQC integrated with a PV system, aimed at enhancing PQ in the electrical grid [1], [2]. The UPQC system consists of a PV array, a series converter, a shunt converter, a filter, an ANFIS-PID control unit, a nonlinear load, and an injecting transformer. These components work together to mitigate power quality issues and reactive power unbalance.

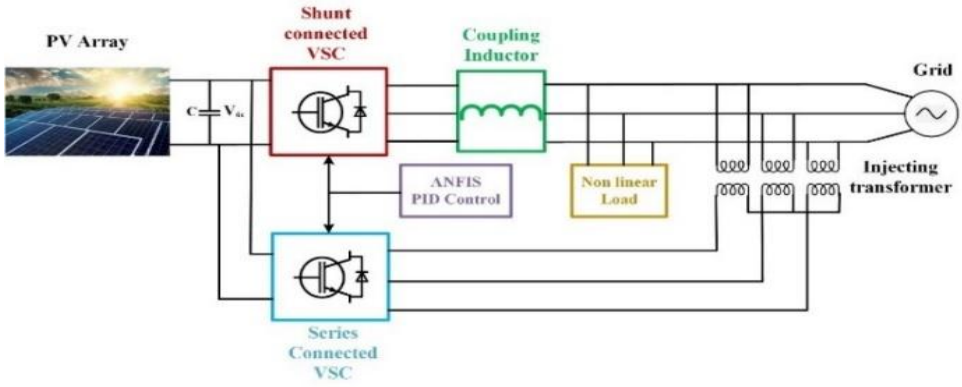

Fig. 1. Block diagram of the proposed system

The PV array generates DC power from solar energy. The series VSC is accountable for injecting compensating voltage to address issues like sags, swells, and harmonic distortion caused by the nonlinear load. By working in coordination with the shunt VSC, the series VSC contributes to stabilizing the voltage supplied to the grid. To ensure that the

injected power is free of high-frequency harmonics, the system includes a filter. This filter smooths out the power output, ensuring that the grid receives clean and stable voltage and current. The ANFIS-PID control unit, which combines ANFIS intelligence with PID control, enables real-time adjustments to the series and shunt converters. This adaptive control allows the system to respond dynamically to disturbances in power quality and varying load conditions, optimizing system performance and stability. The shunt converter plays a key role in reactive power compensation and harmonic mitigation. It manages the flow of reactive power by injecting or absorbing it as needed, which helps balance the current profile and maintain a stable DC link voltage. This DC link, represented by a capacitor, connects the series and shunt converters and ensures a steady flow of power between them. The nonlinear load in the system introduces harmonics and causes fluctuations that can affect power quality. The UPQC, through its control over the series and shunt converters, counteracts these issues, effectively stabilizing the voltage and current given to the grid. Finally, the injecting transformer serves as the connection point between the UPQC system and the grid, transferring the adjusted voltage and current to the grid to ensure optimal power quality [8-10].

2.1. Design of PV-UPQC

Choosing the right sizes for the PV array, DC-link capacitor, and DC-link voltage parameters is the initial step in designing the PV-UPQC system. Reactive power and harmonic currents in the load must be compensated for by the shunt compensator, which must be sized to support the PV modules maximum power output. The UPQC's DC-link and the PV array are directly connected, hence the PV array needs to be set up such that its MPP voltage equals the necessary DC link voltage. When the PV array is performing normally, its capacity is intended to export additional power to the electrical grid in addition to providing the active electricity expected by the load. The DC link voltage (V_{dc}) magnitude is determined by both the modulation depth and the phase voltage. For proper operation, the V_{dclink} must be greater than twice the peak value of the three-phase system's per-phase voltage.

This relationship is particularly important when the modulation (m) is set to 1, The voltage is given in Eq. (1) as follows:

$$V_{dc} = \frac{2\sqrt{2}V_{LL}}{\sqrt{3}m} \quad (1)$$

The sizing of the DC-link capacitor involves both power requirements and DC-bus voltage levels. The power balance equation for the DC-bus capacitor considers several parameters: The C_{dc} is given by Eq. (2).

$$C_{dc} = \frac{3kaV_{ph}I_{sh}t}{0.5\,(V_{dc}^2 - V_{dc1}^2)} \quad (2)$$

Where, Vdc is the DC-bus voltage, Vdc1 is required DC-bus voltage, Overloading factor (a), Per-phase voltage (V_{ph}), Minimum stabilization time after disturbance (t), Per-phase current of the shunt compensator (I_{sh}), Dynamic energy variation factor (k)

The sizing of the shunt compensator's interfacing inductor is given in Eq. (3) determined by three critical parameters: current ripple, switching frequency, and DC-link potential.

$$L_f = \frac{\sqrt{3}mV_{dc}}{12\,af_{sh}I_{rc}} \quad (3)$$

The calculation of the interfacing inductor value incorporates several key factors including the depth of modulation (m), maximum overload expressed in per unit value (a), switching frequency (f_{sh}), and peak-to-peak inductor ripple current (I_{rc}). To minimize harmonic content in the series compensator's operation, its modulation index should be maintained close to unity. This necessitates the use of a series transformer with a specific turn's ratio. The design of the series compensator's interfacing inductor is given in Eq. (4) influenced by three key factors, Ripple current during swell conditions, Switching frequency, DC link voltage.

$$L_r = \frac{\sqrt{3}mV_{dc}K_s}{12af_{se}I_{rc}} \quad (4)$$

Where, Modulation depth (m), Maximum overload in per unit value (a), Switching frequency (f_{se}), Inductor current ripple (I_{rc}).

CONTROL STRATEGY OF PV-UPQC

3.1. ANFIS-PID control

PID controller

The most widely used digital control technique is PID controllers. They are strongly favored because of their resilience and simplicity of use. PID controllers employ an error signal to produce derivative, integral, and proportional signals, which are then added together to produce plant feedback. Eq. (5) provides the PID controller's mathematical model [5-7].

$$u = k_p e + k_i \int e dt + k_d \frac{de}{dt} \quad (5)$$

The proportional, integral, and derivative PID constants are indicated by K_p, K_i, and K_d, respectively. The controller output is denoted by u, and the controller input error signal by e. Although the generated coefficients are not ideal, the Ziegler–Nichols tuning approach is commonly used to adjust the PID controller's settings. This method enables rapid and satisfactory gains and controller responsiveness. Finding the ideal parameters is a challenging task. Moreover, PID controllers' intrinsic linearity and varying performance with non-linear systems represent still another disadvantage.

ANFIS

ANFIS is the combination of NN & Fuzzy, it comprises of 5 different layers, the details of the layer is given as follows. Fuzzification takes place in the input layer, in this instance, a membership value is assigned to each subset inside a fuzzy framework that defines a discourse region for an input. The mathematical framework for this job is given by Eq. (6).

$$o_{ij}^{(1)} = \mu_j(I_{ij}^{(1)}) \quad (6)$$

In Layer 2, known as the fuzzy AND operation layer, each node utilizes the T-norm operator of the algebraic product to perform fuzzy AND operations. The output of each node in this layer is computed using Eq. (7), which calculates the firing strength of each rule as the product of the outputs from the previous layer.

$$o_k^{(2)} = \omega_k = \prod_{i=1}^{q} o_{ij}^{(1)} \quad (7)$$

In Layer 3, referred to as the normalizing layer, the firing strength of each fuzzy rule is normalized by dividing the individual firing strength by the sum of the firing strengths of all the rules in the fuzzy system. This ensures that the activation values of all fuzzy rules are normalized. The normalized output for the kth node is determined using Eq. (8).

$$o_k^{(3)} = \overline{\omega_k} = \frac{o_k^{(2)}}{\sum_{m=1}^{y^2} o_m^{(2)}} \quad (8)$$

Layer 4 is the part of the layer that has constant parameters. The function that each node k in this layer performs is shown in Eq. (9) as a linear product of its inputs, each of which is determined by a set of adjustable parameters (d_{1k}, d_{2k}, d_{yk}, d_o).

$$o_k^{(4)} = \overline{\omega_k} f_k = \overline{\omega_k} \left(d_{1k} I_1^{(1)} + d_{2k} I_2^{(1)} + \cdots + d_{yk} I_y^{(1)} + d_0\right) \quad (9)$$

The output layer, or Layer 5, is where a single node aggregates all entering inputs algebraically to produce the network's output is given by Eq. (10).

$$U_a = o^5 = \sum_{k=1}^{y^2} o_k^{(4)} = \sum_{k=1}^{y^2} \overline{\omega_k} f_k = \frac{\sum_{k=1}^{y^2} \omega_k f_k}{\sum_{k=1}^{y^2} \omega_k} \quad (10)$$

3.1. ANFIS-PID control

The ANFIS is used to tune a PID controller by automatically adjusting the PID parameters (K_p, K_i, and K_d) to improve system performance. Initially, the control objectives for the PID controller are defined. These objectives typically include minimizing the error (difference between the reference and actual output), achieving a fast response time, and reducing overshoot and oscillations. ANFIS is then trained to meet these control objectives by adjusting the PID

parameters. To begin tuning, ANFIS is trained with input-output data from the system. This data consists of the error signal and possibly the change in error. The input data to ANFIS can includes Error (e) & Change in Error (Δe).

ANFIS uses this data to learn the relationship between these inputs and the optimal PID parameters (K_p, K_i, and K_d) for minimizing the error ANFIS applies a hybrid learning algorithm that combines gradient descent (for adjusting fuzzy parameters) and least-squares estimation (for adjusting weights in the neural network). During training, ANFIS continuously adjusts the fuzzy membership functions and the rule parameters to minimize the output error. This hybrid approach allows ANFIS to refine the fuzzy rules and membership functions to achieve optimal PID tuning. After training, ANFIS generates optimal values for K_p, K_i, and K_d based on real-time error and change in error. This means that the PID controller's parameters are no longer fixed but are dynamically updated based on the system's performance and operating conditions. ANFIS effectively acts as a supervisory control layer over the PID controller, adapting it to varying conditions [3], [4], [11], [16].

3.2. Control of series compensator

The control logic for the series compensator in the UPQC system is shown in Fig. 2. It represents the series control of a UPQC, designed to maintain voltage quality by compensating for disturbances such as sags, swells, and harmonics. The system utilizes a Phase PLL to synchronize with the grid and extract the grid's phase angle for dq0 transformations. The grid voltages (V_{sa}, V_{sb}, V_{sc}) and load voltages (V_{La}, V_{Lb}, V_{Lc}) are transformed from the three-phase (abc) system into the dq0 reference frame. The direct and quadrature components (V_{Ld}, V_{Lq}) of the load voltage are compared with their respective reference values, where V_{Ld}* is typically set to 0 to ensure balanced voltage compensation. The resulting errors are processed through ANFIS-PID controllers, which calculate the required compensating voltage in the dq frame [12],[14], [17-19]. The reference compensating voltages (V_{SEd}, V_{SEq}) are then transformed back to the abc frame for the series converter. A SVPWM voltage controller generates the switching pulses to drive the series converter, which injects compensatory voltages (V_{SEa}, V_{SEb}, V_{SEc}) into the system. This compensates for any voltage disturbances at the load end, ensuring the load receives clean and stable power. The integration of ANFIS with the PID controller improves dynamic response and adaptability, while the SVPWM ensures efficient and precise voltage control.

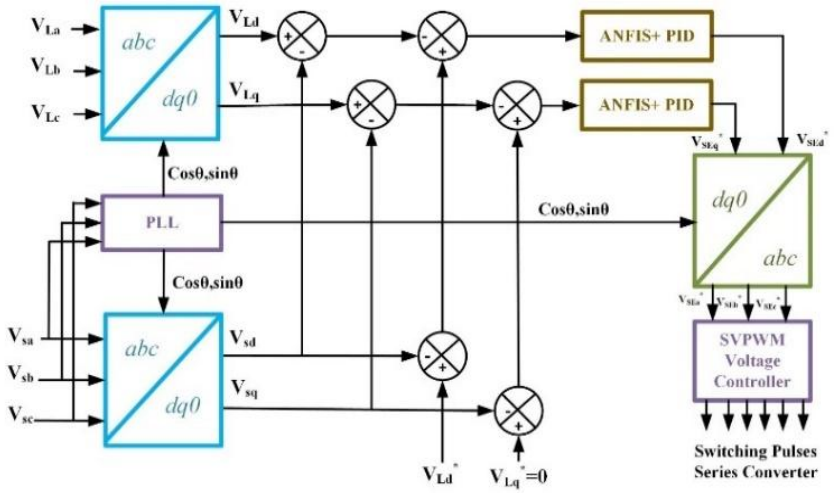

Fig. 2. Control logic of series compensator

3.3. Control of shunt compensator

Fig.3 represents the shunt control mechanism of a UPQC. It operates by ensuring power quality at the load side by compensating for current-related disturbances such as harmonics and reactive power. At its core, a Phase Locked Loop (PLL) synchronizes the system with the grid by extracting the grid's phase angle. The load currents (i_{La}, i_{Lb}, i_{Lc}) are converted from the three-phase system (abc) to a two-axis reference frame (dq0) to isolate the direct and quadrature components. The direct current (I_{Ld}) undergoes filtering via a Moving Average Filter to remove high-frequency noise, resulting in I_{Ldf}. This filtered current is then used to calculate the reference current (I_{sd}*) after compensating for losses using an ANFIS combined with a PID controller, which provides precise control for dynamic performance improvements.

The shunt converter utilizes a Hysteresis Current Controller to generate switching pulses for maintaining the desired current waveform. The reference current components are transformed back to the three-phase domain (abc) for injecting compensatory currents (i_{sa}, i_{sb}, i_{sc}) into the system. The MPPT module ensures optimal power extraction from the PV system, providing a steady V_{dc}. This voltage is processed through a Moving Average Filter to stabilize fluctuations before being compared to the desired reference voltage (V_{dc}*). The resultant error drives the control loop, maintaining the DC-link voltage and supporting seamless power quality enhancement in the grid-connected PV-UPQC system. The integration of ANFIS improves adaptability, while the Hysteresis Controller ensures fast response, making the system highly effective in addressing harmonic and reactive power issues [20].

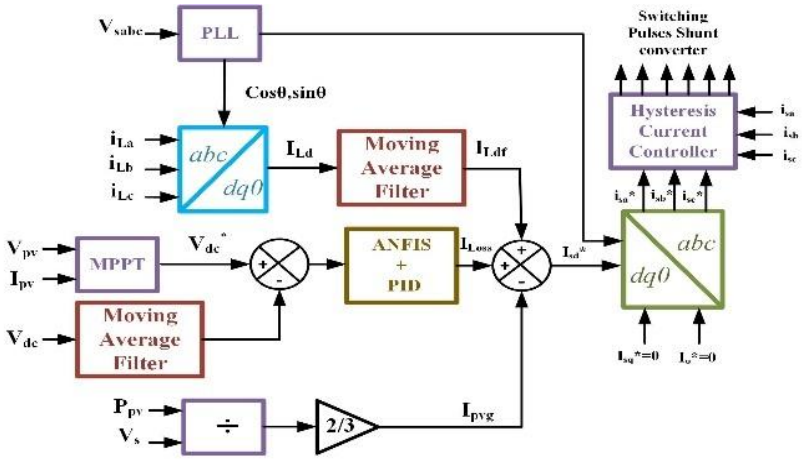

Fig. 3. Control logic of shunt compensator

3.4. SVPWM Control

The primary objective of SVPWM is to generate a sinusoidal voltage waveform at the output of the inverter while maximizing the utilization of the DC bus voltage, reducing harmonic distortion, and improving system efficiency. An inverter has six active switching states and two zero states, which together define a hexagonal voltage space. These states can be visualized as six active voltage vectors and two zero vectors in a two-dimensional plane. SVPWM operates by dynamically synthesizing a reference voltage vector V_{ref} within this hexagonal space. To achieve the desired voltage and frequency output, V_{ref} is approximated as a combination of two adjacent active vectors and one zero vector in every switching cycle. This combination allows the inverter to closely match the magnitude and angle of V_{ref} over time, creating an effective sinusoidal waveform [13].

The reference voltage vector is expressed in terms of its magnitude and angle θ relative to the active voltage vectors. The time durations for which each vector is applied in a switching period T_s are calculated in Eq. (11) and Eq. (12) as follows:

$$T_1 = \frac{\sqrt{3}T_s}{V_{dc}} \left| V_{ref} \sin\left(\frac{\pi}{3} - \theta\right) \right| \quad (11)$$

$$T_2 = \frac{\sqrt{3}T_s}{V_{dc}} \left| V_{ref} \sin(\theta) \right| \quad (12)$$

T_1 & T_2 are the time durations for the two adjacent active vectors
T_0 is the time for the zero vector,
T_s is the total switching period
θ is the angle of V_{ref}

The three-phase voltages (V_a,V_b,V_c) generated by the inverter correspond to specific switching states. SVPWM operates in the two-dimensional space defined by the Clarke Transformation, which converts the three-phase voltages into two orthogonal components (V_α) and (V_β) in a stationary αβ-frame. This approach simplifies the analysis and modulation.

The relationship is expressed using the Clarke Transformation

$$\begin{bmatrix} V_\alpha \\ V_\beta \end{bmatrix} = \frac{2}{3}\begin{bmatrix} 1 & -\frac{1}{2} & -\frac{1}{2} \\ 0 & \frac{\sqrt{3}}{2} & -\frac{\sqrt{3}}{2} \end{bmatrix}\begin{bmatrix} V_a \\ V_b \\ V_c \end{bmatrix} \quad (13)$$

In Eq. (13), V_a,V_b,V_c are the Three-phase voltages, V_α,, V_β: Components in the αβ-plane. The V_{ref} is synthesized as a combination of active voltage vectors and zero vectors. In this proposed scheme, the SVPWM generate the switching pulses to the VSC present in the UPQC. The switching pulses to the corresponding VSC is controlled using the ANFIS PID Controller.

RESULTS AND DISCUSSION

The Simulation of the proposed scheme is carried out considering the three cases, The Simulink model of the scheme is presented in the Fig. 4.

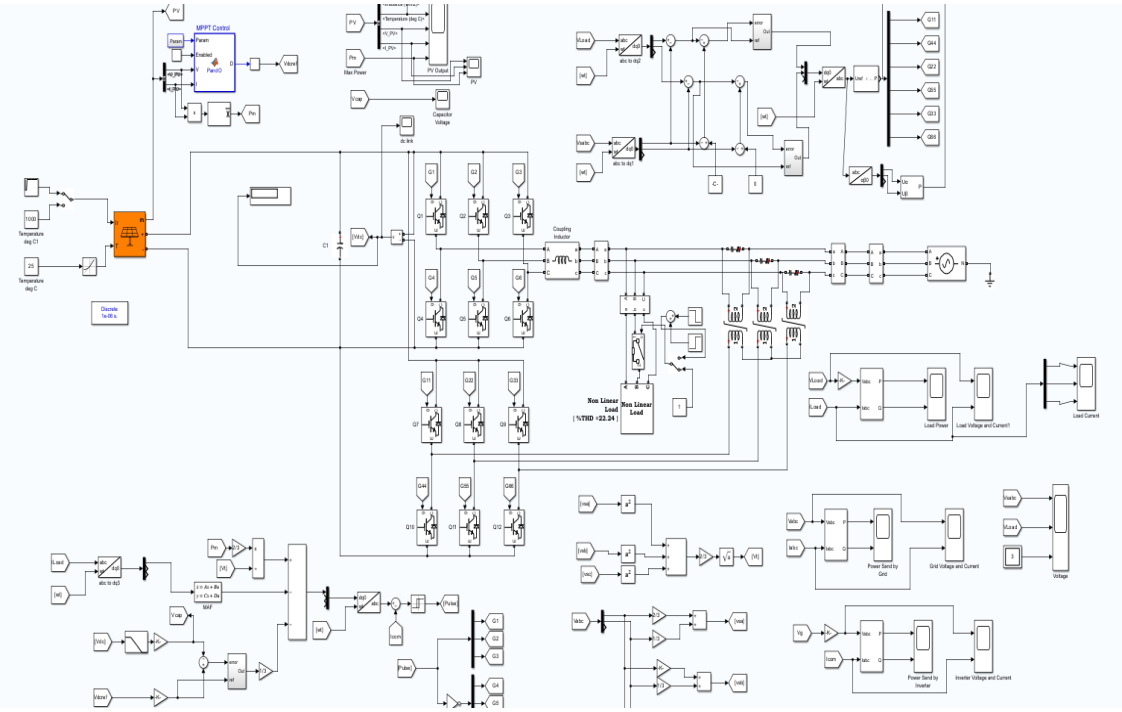

Fig. 4. Simulink Model of the proposed work

Case-1 Variation in irradiance of pv

In this case, the irradiance of the PV is varied, the variation in irradiance & temperature is represented in the Fig.5. The PV parameters is shown in the Fig.6. The power obtained from the PV is 47.12 KW during irradiance of 500 W/m² & 90.49 KW at 1000 W/m².the temperature of the PV is maintained at 25°C.

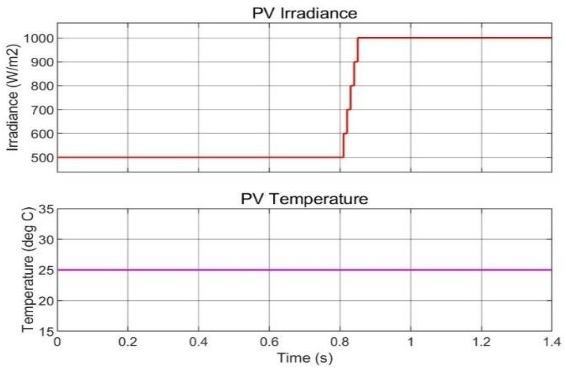

Fig. 5. PV irradiance & temperature

The grid parameters are represented in Fig. 7. When the irradiance of the PV is less, the grid receives less power. When the irradiance of the PV is increased, the grid receives more power. The load parameters are presented in Fig. 8, in which they are maintained constant. Fig. 9 represents the voltage of the grid, load, and UPQC during varying irradiance conditions. As there is no PQ issued, no voltage is injected from the UPQC. The shunt inverter voltage and current are represented in Fig. 10. The DC link voltage is denoted in Fig. 11, it is maintained around 657 V.

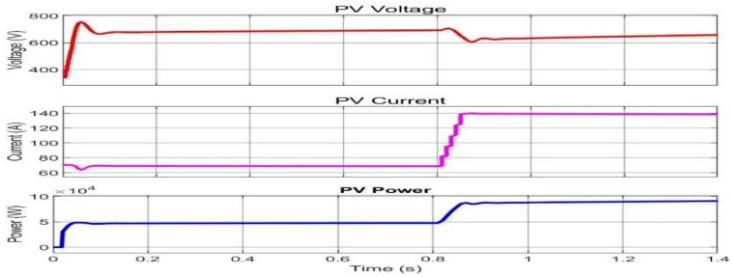

Fig. 6. PV parameters during case-1

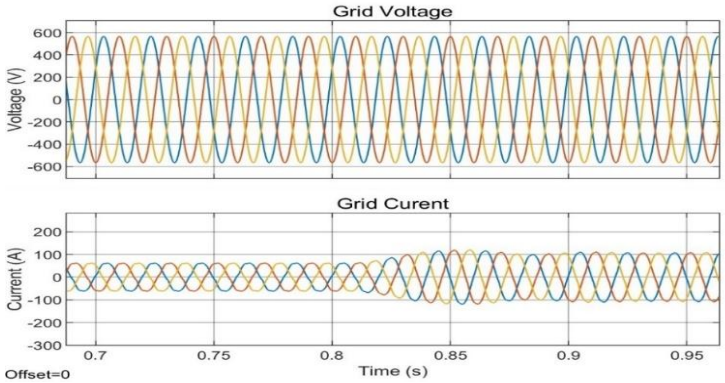

Fig. 7. Grid voltage & current during case-1

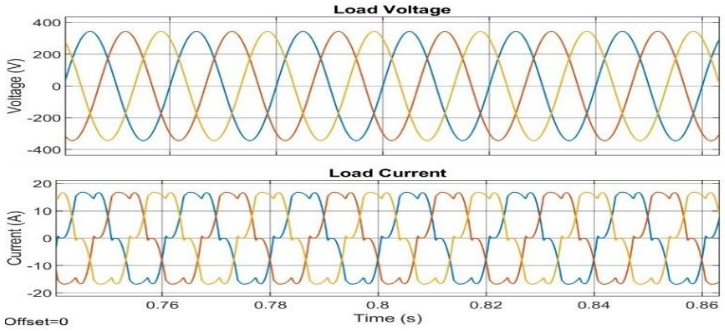

Fig. 8. Load voltage & current during case-1

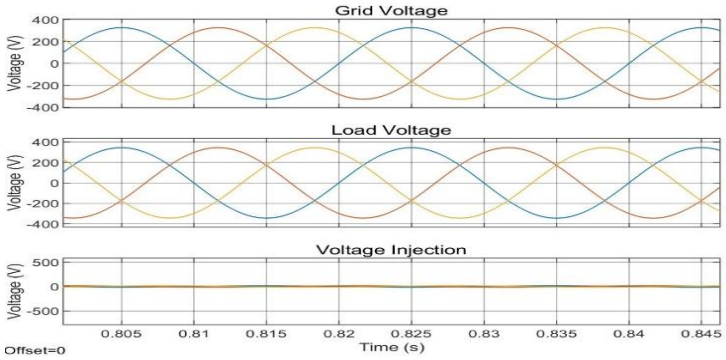

Fig. 9. Voltage of grid, load & injected voltage by UPQC during case-1

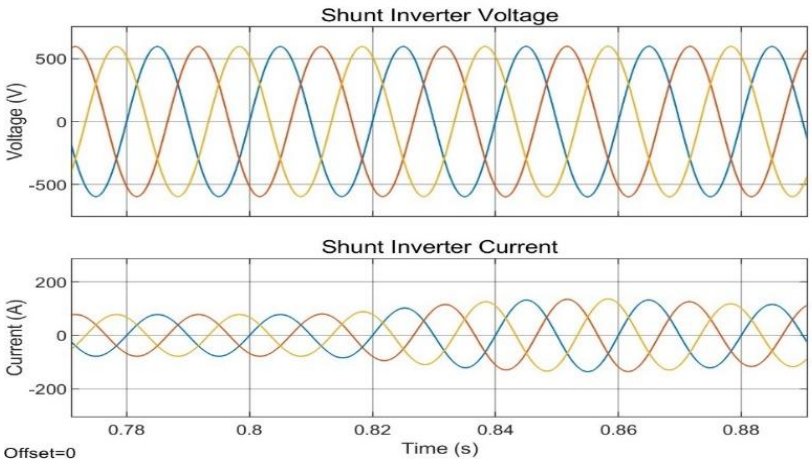

Fig. 10. Shunt inverter voltage & current during case-1

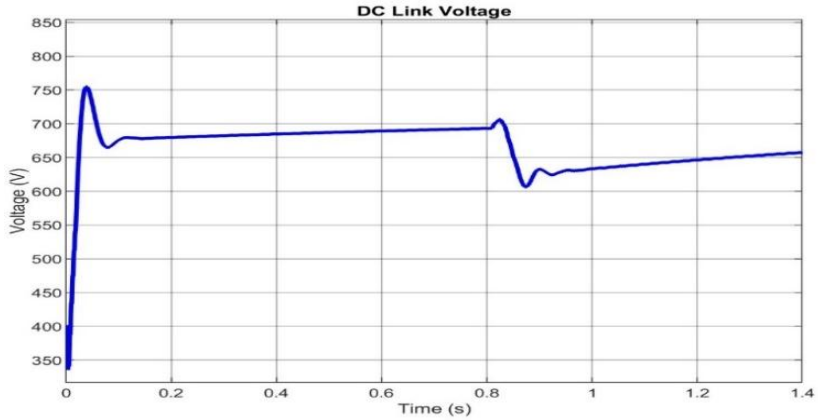

Fig. 11. DC link voltage during case-1

Case-2 During power quality issues

In this case, PQ issues were considered: voltage sag is created from 0.7 to 0.85s and voltage swell is from 1 to 1.25 seconds. Here the PV is operating with full irradiance and the load is constant. Fig.12 represents the voltage of grid, load, and injected voltage during sag. Here it is evident that the grid voltage is reduced from 0.7 to 0.85 seconds. To compensate the voltage and maintain the load voltage constant, UPQC will inject the required voltage to balance the sag in the grid. In the same way, voltage swell is occurring from 1 to 1.25 s. To keep the load voltage stable. The series compensator injects the required voltage through the transformer. In both cases, the load voltage is retained constant. Fig. 13 represents the voltage of the grid, load, and injected voltage during sag. The voltage and current of the grid and shunt inverters are represented in Fig. 14 and Fig.15, respectively. The load details are displayed in Fig. 16. The DC link voltage obtained during this case is denoted in Fig. 17. Here the DC link potential is maintained around 670V.

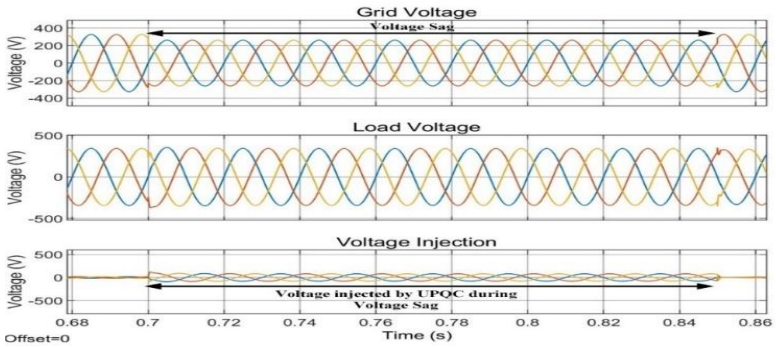

Fig. 12. Voltage of grid, load & injected voltage by UPQC during sag

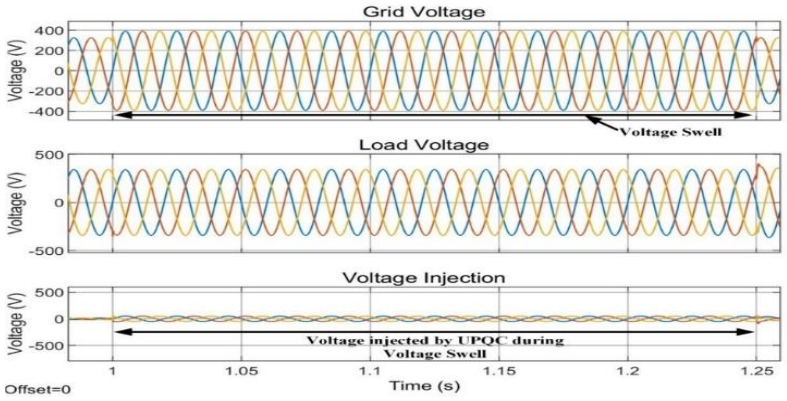

Fig. 13. Voltage of grid, load & injected voltage by UPQC during swell

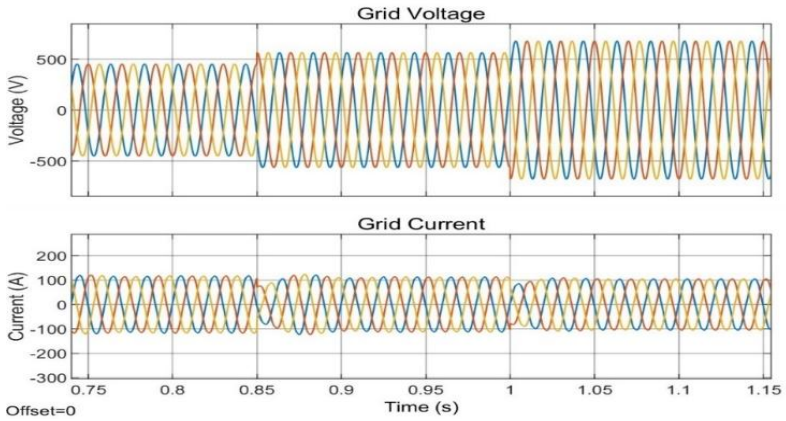

Fig. 14. Grid parameters during case-2

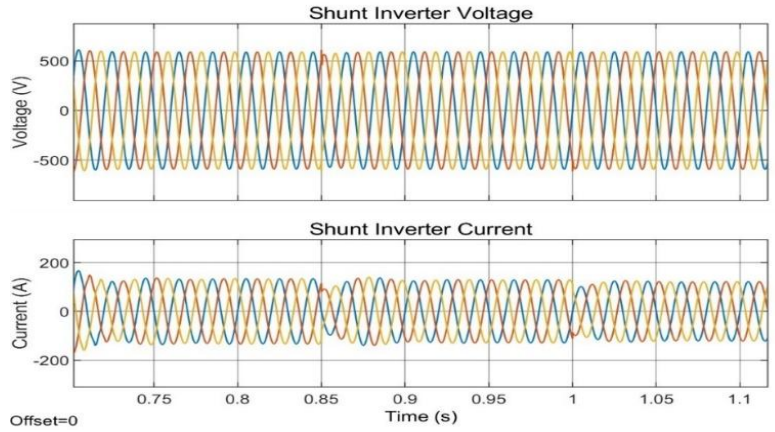

Fig. 15. Grid parameters during case-2

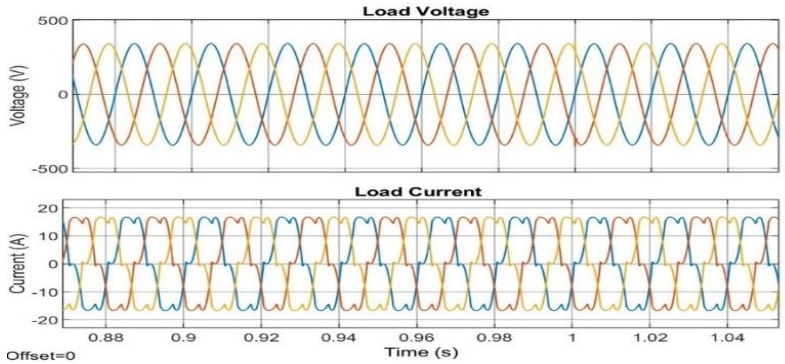

Fig. 16. Load parameters during case-2

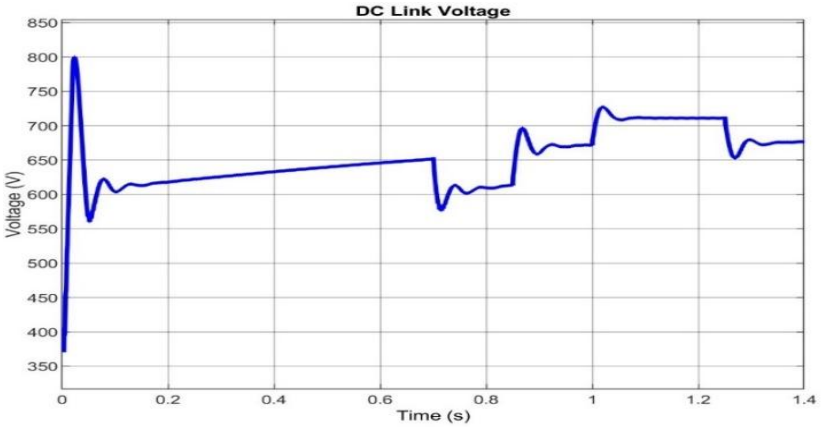

Fig. 17. DC link voltage during case-2

Case-3 During unbalanced load condition

In this case, Voltage unbalance is created in the load, the representation of the voltage unbalance in phase-b from 1 to 1.2 s is presented in the Fig.18. The load voltage & Current is explained in the Fig.19. The variation in load unbalance is represented from 1 to 1.2s.

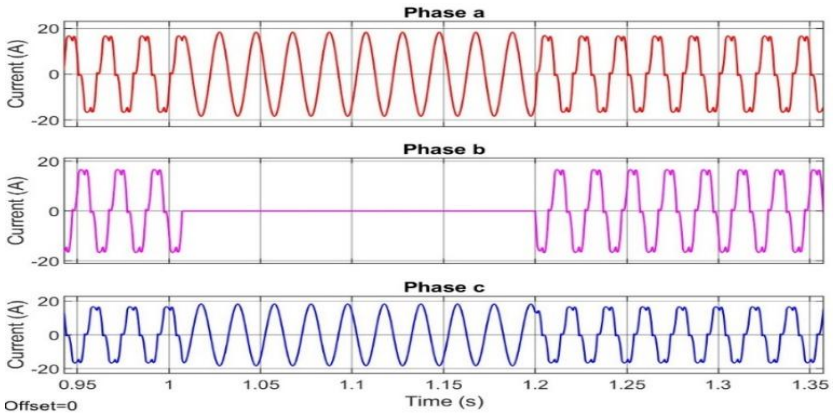

Fig. 18. Representation of load unbalance in phase-b

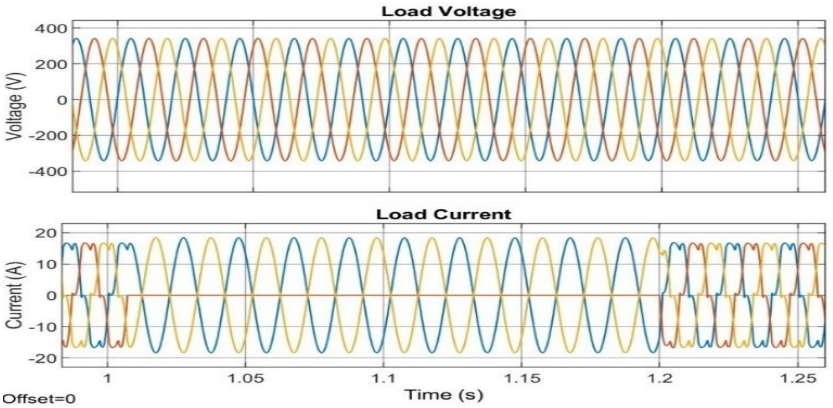

Fig. 19. Load voltage & current during case-3

Fig. 19 represents the load voltage & Current during case-3, Here the load current represents the unbalanced load condition due to the phase-b. The Voltage & Current of grid & shunt inverter are described in Fig. 20 & Fig. 21 respectively. The DC link voltage during case-3 is represented in Fig. 22. The DC link voltage is maintained at around 680 V.

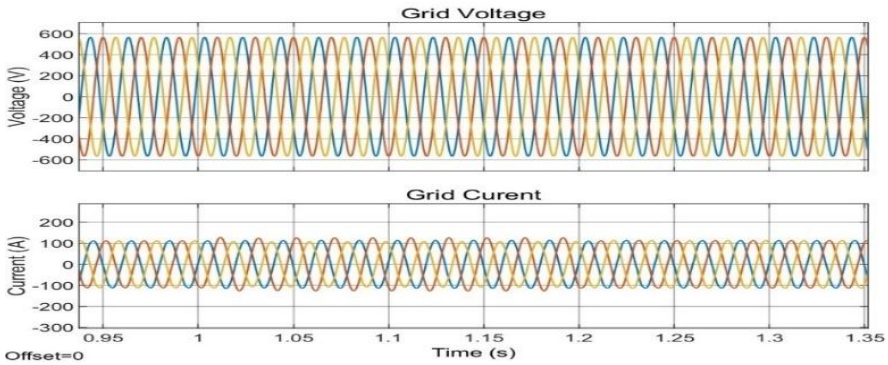

Fig. 20. Grid voltage & current during case-3

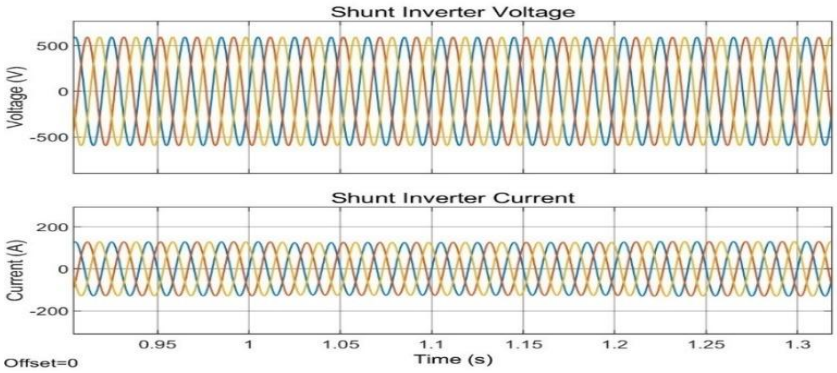

Fig. 21. Shunt inverter voltage & current during case-3

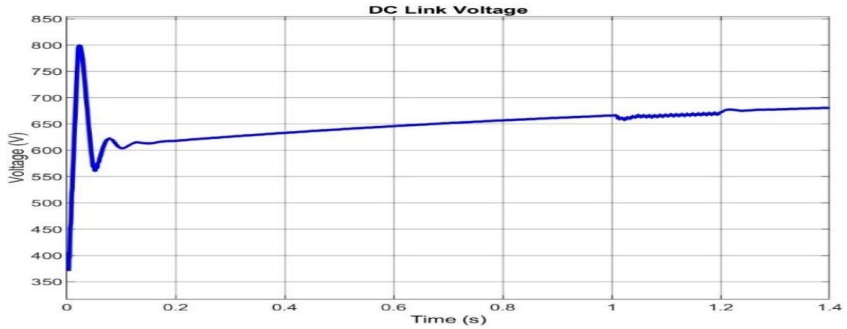

Fig. 22. DC link voltage during case-3

THD analysis

Case 1

The THD analysis during case-1 is represented in Fig. 23. The THD obtained is 0.01% for load voltage presented in Fig. 23 (a) & 2.69% for Grid current given in Fig. 23 (b) respectively.

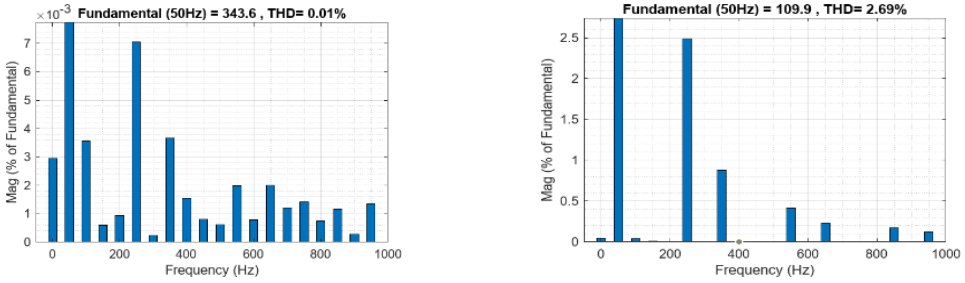

(a) (b)

Fig. 23. THD during case-1 (a) load voltage (b) grid current

Case-2

The THD analysis of Case 2, considering the power quality (PQ) disturbance voltage sag is presented in Fig. 24. The THD obtained is 0.01% for load voltage presented in Fig. 24 (a) & 2.49% for Grid current given in Fig. 24 (b) respectively. Similarly, the THD during a voltage swell is shown in Fig. 25, The THD obtained is 0.01% for load voltage presented in Fig. 25 (a) & 2.78% for Grid current in Fig. 25 (b) respectively.

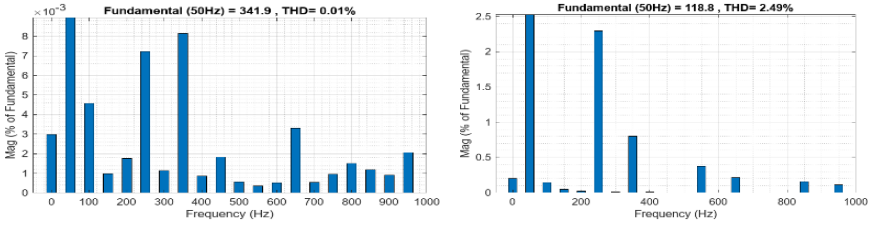

(a) (b)

Fig. 24. THD during case-2 (voltage sag) (a) load voltage (b) grid current

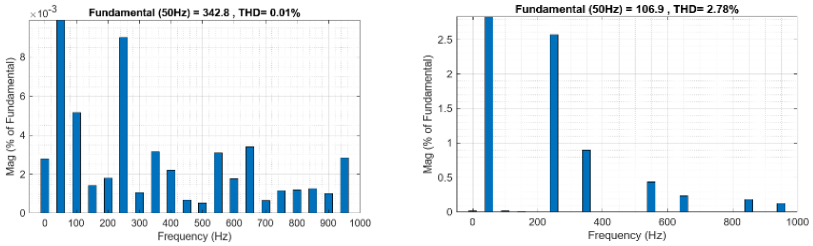

(a) (b)

Fig. 25. THD during case-2 (voltage swell) (a) load voltage (b) grid current

Case-3

The THD analysis of case-3 is represented in Fig. 26. The THD obtained is 0.01% for load voltage presented in Fig. 26 (a) & 2.49% for Grid current in Fig. 26 (b) respectively.

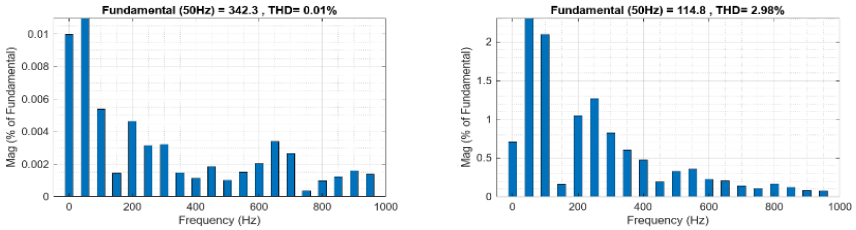

(a) (b)

Fig. 26. THD during case-3 (load unbalance) (a) load voltage (b) grid current

In all the above THD analysis, the THD is minimal & ANFIS-PID control provide the optimal performance of the proposed scheme. In all the above cased the V_{dclink} is maintained between 650 to 700 V.

Comparative analysis of the proposed system

Table 1 presents the gain values for different PID controller configurations paired with MPPT techniques. These include a simple PI controller with MPPT, a PID controller with MLNN, and PID controllers integrated with both MLNN and Bacterial Foraging Optimization (BFO) for MPPT. The proposed approach, combining PID with ANFIS, uses balanced gain values of ($K_p = 1$), ($K_i = 1$), and a small ($K_d = 0.01$). This configuration aims to leverage ANFIS for its adaptability, achieving a fine-tuned response with minimal overshoot.

Table 1 PID controller gain values

Gain parameter	K_p	K_i	K_d
PI + MPPT	2.5	1.1	-
PID + MLNN	1.32	2.74	1.56
PID + MLNN with BFO MPPT	0.98	0.92	0.93
Proposed (PID + ANFIS)	1	1	0.01

Table 2 compares the stability of the DC link voltage for each method. The (PID+MLNN) controller achieves a voltage range of 720-780 V, showing moderate fluctuation. Adding the BFO optimization to (PID+MLNN) reduces the voltage range to 720-750 V, indicating improved control stability. The proposed (PID+ANFIS) setup shows even more refined control, with the DC link voltage maintained within 660-700 V. This narrow range demonstrates ANFIS's capability to consistently regulate voltage under varying conditions.

Table 2 Comparison of dc link voltage

Method	Range of dc link voltage
PID + MLNN	720-780 V
PID + MLNN with BFO MPPT	720-750 V
Proposed (PID+ANFIS)	660-700 V

The proposed (PID+ANFIS) method outperforms other approaches by maintaining the DC link voltage around 700 V with minimal variation, proving it to be a robust and reliable solution. This ANFIS-enhanced controller's ability to stabilize voltage across different scenarios makes it an ideal choice for applications requiring precise voltage regulation.

CONCLUSION

The proposed system effectively addresses power quality issues and enhances grid performance under varying operating conditions. During variations in irradiance, the system ensures consistent power delivery and maintains the DC link voltage around 657 V. Under power quality disturbances like voltage sags and swells, the Unified Power Quality Conditioner (UPQC) compensates for voltage deviations, maintaining stable load voltage. During unbalanced load conditions, the system demonstrates robust performance by maintaining voltage stability despite phase imbalances. The THD analysis confirms minimal distortion in all cases, with load voltage THD at 0.01% and grid current THD below 2.78%, showcasing the effectiveness of the ANFIS-PID control scheme. The system maintains a consistent DC link voltage between 650 to 700 V across all scenarios, validating the reliability and efficiency of the proposed approach.

Future Scope

The proposed system can be extended to incorporate advanced optimization techniques and machine learning algorithms for further enhancing system efficiency and adaptability under dynamic conditions. Future research could focus on integrating hybrid renewable energy sources, such as wind and fuel cells, with the existing PV system to create a more robust hybrid energy model. Additionally, real-time implementation of the proposed scheme in a larger-scale microgrid with multiple distributed energy resources and varying load profiles can provide valuable insights into its scalability and practical feasibility. Incorporating vehicle-to-grid (V2G) technology and energy storage systems like supercapacitors could further improve grid stability and energy utilization.

Declaration of Competing Interest

The authors declare no conflict of interest, financial or otherwise.

Data Availability

The data and supportive information are available within the article.

REFERENCES

[1] Devassy, S., & Singh, B. (2017). "Design and performance analysis of three-phase solar PV integrated UPQC". IEEE Transactions on Industry Applications, 54(1), 73-81. https://doi.org/ 10.1109/TIA.2017.2754983

[2] Vignesh, T., & Hariharan, R. (2022, December). "Design and performance analysis of three phase solar PV integrated UPQC". In AIP Conference Proceedings (Vol. 2426, No. 1). AIP Publishing. https://doi.org/10.1063/5.0127331

[3] Srilakshmi, K., Sujatha, C. N., Balachandran, P. K., Mihet-Popa, L., & Kumar, N. U. (2022). "Optimal design of an artificial intelligence controller for solar-battery integrated UPQC in three phase distribution networks". Sustainability, 14(21), 13992. https://doi.org/10.3390/su142113992

[4] Srilakshmi, K., Rao, G. S., Swarnasri, K., Inkollu, S. R., Kondreddi, K., Balachandran, P. K., & Colak, I. (2024). "Optimization of ANFIS controller for solar/battery sources fed UPQC using a hybrid algorithm". Electrical Engineering, 1-28. https://doi.org/10.1007/s00202-023-02185-8

[5] Yadav, S. K., & Yadav, K. B. (2024). "Performance analysis of hybrid metaheuristic assisted collateral FO controller for HRES system integrated UPQC". Computers and Electrical Engineering, 120, 109664. https://doi.org/10.1016/j.compeleceng.2024.109664

[6] Rafiqi, I. S., & Bhat, A. H. (2024). "Enhancement of power quality using UPQC integrated with renewable energy sources through an improved sparrow search-based PID controller". International Journal of Advanced Technology and Engineering Exploration, 11(116), 955. https://dx.doi.org/10.19101/IJATEE.2023.10102395

[7] Nagaraju, S., & Bethi, C. (2024). "CGA-Fopid Based UPQC for Mitigating Harmonics and Compensate Load Demand in Grid Linked Hybrid Renewable Energy SOURCES". Suranaree Journal of Science & Technology, 31(1). https://doi.org/10.55766/sujst-2024-01-e02177

[8] Bharat Mohan, N., Rajagopal, B., & Hari Krishna, D. (2023). "Power quality enhancement of hybrid renewable energy source-based distribution system using optimised UPQC". Journal of Control and Decision, 1-22. https://doi.org/10.3390/fractalfract8030140

[9] Nkado, F., Nkado, F., Oladeji, I., & Zamora, R. (2021). "Optimal design and performance analysis of solar PV integrated UPQC for distribution network". European Journal of Electrical Engineering and Computer Science, 5(5), 39-46. https://doi.org/10.24018/ejece.2021.5.5.361

[10] Mansor, M. A., Hasan, K., Othman, M. M., Noor, S. Z. B. M., & Musirin, I. (2020). "Construction and performance investigation of three-phase solar PV and battery energy storage system integrated UPQC". Ieee Access, 8, 103511-103538. https://doi.org/10.1109/ACCESS.2020.2997056

[11] Jadhav, R. S., & Mallareddy, C. H. (2019). "Artificial neural network-based design and performance of three-phase solar PV integrated UPQC". International Journal of Industrial Electronics and Electrical Engineering, 228-237.

[12] Dhagate, D. R., Dhamaal, S. S., & Thakre, M. P. (2020, December). "Design and performance evaluation of 3-phase photovoltaic integrated UPQC". In 2020 international conference on power, energy, control and transmission systems (ICPECTS) (pp. 1-7). IEEE.https://doi.org/10.1109/ICPECTS49113.2020.9337053

[13] Sandhya, J., & Sirisha, N. (2020). "Performance analysis of three-phase solar PV integrated UPQC using space vector technique". Journal of Science & Technology (JST), 5(5), 140-148. https://doi.org/10.46243/jst.2020.v5.i5.pp140-148

[14] Devassy, S., & Singh, B. (2020). "Performance analysis of solar PV array and battery integrated unified power quality conditioner for microgrid systems". IEEE Transactions on Industrial Electronics, 68(5), 4027-4035. https://doi.org/10.1109/TIE.2020.2984439

[15] Kumar, A., & Jain, R. (2017). "Implementation and Performance Evaluation of Three Phase Solar PV-UPQC for Power Quality Enhancement". International Journal of Engineering and Management Research (IJEMR), 7(3), 744-751. https://doi.org/10.1109/ICOSEC51865.2021.9591823

[16] Vijay, M. V. U. M. A., Buda, S. K., Kumar, Y. A., Abraham, M., Sreelekha, D., & Ratnakar, M. (2022). "Design and Performance Monitoring of Artificial Neural Network based Three-Phase Solar PV System with Integrated UPQC". NeuroQuantology, 20(10), 9658. https://doi.org/10.14704/nq.2022.20.10.NQ55943

[17] Bhalchandra Kalaskar, K., Ghuge, K., & Unde, M. G. (2021, October). "Implementation of three phase photo voltaic (PV) integrated unified power quality conditioner (UPQC)". In 2021 2nd International Conference on Smart Electronics and Communication (ICOSEC) (pp. 1-4). IEEE. https://doi.org/10.1109/ICOSEC51865.2021.9591823

[18] Ray, P., Ray, P. K., & Dash, S. K. (2021). “Power quality enhancement and power flow analysis of a PV integrated UPQC system in a distribution network”. IEEE Transactions on Industry Applications, 58(1), 201-211. https://doi.org/10.1109/TIA.2021.3131404

[19] Mohan, H. M., Dash, S. K., Ram, S. K., & Caesarendra, W. (2022, July). “Performance assessment of three-phase PV tied NPC multilevel inverter based UPQC”. In 2022 International conference on intelligent controller and computing for smart power (ICICCSP) (pp. 1-5). IEEE. https://doi.org/10.1109/ICICCSP53532.2022.9862340

[20] Yadav, S. K., & Yadav, K. B. (2022). “Implementation of three-phase hybrid energy system integrated with UPQC”. In Recent Advances in Power Electronics and Drives: Select Proceedings of EPREC 2021 (pp. 305-316). Singapore: Springer Nature Singapore. https://doi.org/10.1007/978-981-16-9239-0_23

[21] Goswami, G., & Goswami, P. K. (2022). ANFIS supervised PID controlled SAPF for harmonic current compensation at nonlinear loads. IETE Journal of Research, 68(5), 3585-3596. https://doi.org/10.1080/03772063.2020.1770134

[22] Odonkor, E. N., Moses, P. M., & Akumu, A. O. (2023). Multiple grid-connected microgrids with distributed generators energy sources voltage control in radial distribution network using ANFIS to enhance energy management. International Journal of Electrical and Electronics Research, 11(4), 1188-1203. https://doi.org/10.37391/ijeer.110441

[23] Yadav, S. K., Yadav, K. B., & Priyadarshi, A. (2024). Performance analysis of three-phase solar PV, BESS, and Wind integrated UPQC for power quality improvement. Computers and Electrical Engineering, 116, 109230. https://doi.org/10.1016/j.compeleceng.2024.109230

[24] Sanjenbam, C. D., Shah, P., & Singh, B. (2022). Multi-functional control strategy for power quality improvement of three-phase grid using solar PV fed unified power quality conditioner. IET Energy Systems Integration, 4(4), 518-531. https://doi.org/10.1049/esi2.12077

[25] Dheeban, S. S., & Muthu Selvan, N. B. (2023). ANFIS-based power quality improvement by photovoltaic integrated UPQC at distribution system. IETE Journal of Research, 69(5), 2353-2371. https://doi.org/10.1080/03772063.2021.1888325

[26] Chitra, L., Sridevi, M., & Prakash, S. (2024, August). Intelligent MPPT Controller for PV with Energy Storage System Fed UPQC System for Power Quality Improvement. In 2024 7th International Conference on Circuit Power and Computing Technologies (ICCPCT) (Vol. 1, pp. 1287-1293). IEEE. https://doi.org/10.1109/ICCPCT61902.2024.10672830